Three-Phase Four-Wire Hybrid Active Power Filter for Mitigating Harmonic Problems Caused by CFLs Lamps based on a Shunt Active Power Filter SAPF in Parallel with a Passive Filter

MOHAMED HAJJEJ, LASSAAD SBITA
Process Laboratory, Energetic, Environment and Electrical System (PEESE),
National Engineering School of Gabès (ENIG),
University of Gabès,
TUNISIA

Abstract: - The widespread integration of nonlinear loads across industrial, commercial, and residential settings has significantly exacerbated power quality issues within contemporary power distribution systems. An example of such nonlinear loads is the prevalent use of compact fluorescent lamps (CFLs), intended as replacements for incandescent lamps (ILs). CFLs have gained popularity owing to their reduced energy consumption and extended lifespan, contributing to their extensive use across various applications. But those lamps inject high harmonic current in the power system. To address this issue, a hybrid active power filter HAPF based on a shunt active power filter SAPF in parallel with a passive filter (PF) is implemented in this paper. The reference current is calculated based on the PQ theory, and the voltage source inverter VSI is controlled via a simple hysteresis current controller (HCC). The results show that the PF is suitable to compensate for the Hight harmonic generated by both the load and the switched device of the APF. Also, this HAPF is well designed and implemented to mitigate all harmonic generated by CFL lamps on the power system, and compensate the reactive power. The THD of the current is reduced from 90.75% before compensation to 0.75% after compensation. This implies that the main injects only the Fundamental current to the power.

Key-Words: - Shunt active power filter (SAPF), passive filter (PF), PQ theory, hysteresis current controller (HCC), hybrid active power filter (HAPF), Harmonics, current compensation, THD.

Received: August 13, 2023. Revised: February 7, 2024. Accepted: March 5, 2024. Published: April 8, 2024.

1 Introduction

In recent years, the escalating use of semiconductor devices and nonlinear loads across various applications has made power quality issues a significant concern in power systems. Such as residential or industrial loads and in particular the light loads that represent 25% of the total power loads, [1]. The massive use of Compact fluorescent lamps CFLs injects high harmonic current into the main systems for all harmonic levels, [2]. So, harmonic currents, in particular, have become a major focus in this context. Passive power filters (PFs) primarily composed of inductive and capacitive elements (L-C) are considered the best low-cost solutions that offer fixed current compensation. Diverging from Active Power Filters APFs that provide dynamic and adaptable solutions. They proactively respond to power quality issues, affording precise control while minimizing resonance effects often associated with passive filters. Additionally, Shunt APFs offer advantages in terms of sizing and flexibility, making them the preferred choice for addressing power quality challenges, [3]. Shunt active power filters (SAPFs) are widely employed to manage current harmonics, reactive power compensation, and neutral current compensation in distribution systems. Typically installed at the Point of Common Coupling (PCC) as presented in Figure 1, where nonlinear loads connect with the utility grid, these filters are more adept at mitigating current harmonics compared to passive power filters (PFs), which offer fixed compensation and are limited by factors like resonance effects and specific sizing, [4].

Presently, the attention of researchers and developers is directed toward both the design and control aspects of SAPFs tailored for three-phase four-wire (3ph-4W) nonlinear loads. So, various SAPF topologies have emerged to tackle these challenges, including the four-leg (4L) configuration [5], the split capacitor or two capacitors (2C) approach [6] and the three H-bridges (3-HB)

topology, each H-bridge comprising four switches arranged in an H shape [7], which is illustrated in Figure 2.

In the split capacitor topology, the neutral wire resides between two capacitors, necessitating an additional control loop to maintain the DC voltage balance between the capacitors. In contrast, the 4L configuration introduces two active switches to the fourth leg (neutral wire) to balance the neutral current, resulting in superior performance compared to the 2C topology. This configuration has been extensively explored in various research studies, [8], [9]. Conversely, the 3-HB inverter topology employs three full H-bridges sharing a DC-link capacitor, requiring three single-phase isolated transformers to connect the 3-HB filter to the system and more switches than other configurations.

While those researchers are focusing on optimizing and creating various parallel active filter topologies, others delve into perfecting the control aspect, which represents the "heart" of these filters. The efficacy of the filtering process is closely tied to the reference current extraction algorithm. These methodologies typically fall into two main categories: frequency domain methods and time domain methods.

Frequency domain methods, such as the fast Fourier transform (FFT), extract harmonic components from distorted voltage and current signals. Despite providing precise values of harmonic amplitude and phases, these techniques suffer from aliasing effects, spectral leakage, and slow response times due to heavy computational loads, necessitating complex systems for real-time operation.

Conversely, time domain methods, including the p-q theory, instantaneous reactive power theory, synchronous reference frame theory (SRF), and p-q-r theory, have gained attention. SRF employing a phase-locked loop (PLL) system, ensures undistorted transformation angles even under unbalanced source conditions, enabling its usage for voltage and current reference generation. The reference currents serve as inputs to the power switch control block.

Hysteresis control algorithms (HCA) represent simple and practical techniques for SAPF and power switch device control. HCA operates with two predefined bands, ensuring the modulated currents remain within specified limits, resulting in close tracking of the compensating current to the reference current. HCA determines the VSI (Voltage Source Inverter) switches' "ON" and "OFF" states, leading to straightforward implementation, robustness, and high performance. However, HCA is constrained by a limited frequency range and nonlinear effects. Addressing these limitations, researchers have introduced a new technique called pulse width modulation (PWM) control, which generates a modulation signal to adjust the duty cycle of power electronic switches, [10], in wish is not the subject of this paper.

Moreover, and based on previous experimental and simulation research, we found that the load generates high harmonics for both low and high harmonic levels. Also, it is noticed that the switching devices of the APF may inject some harmonic and in particular high frequency. So, as a solution to mitigate both harmonics generated by CFL and APF in high frequency levels a Hybrid active power filter HAPF is proposed in this paper. The HAPF consists of a second-order high-pass passive filter in parallel with an APF. The overall system is estimated, and implemented by MATLAB Simulink software. This is crucial to comply with relevant national and international harmonic standards, including NTF 15-520 and IEC61000-3-2, [11], [12]. Also, Shunt Active Power Filters can be used in industrial setups where Variable Frequency Drives are employed. VFDs often introduce harmonic distortion into the power system, and SAPFs can help mitigate these harmonics, ensuring a cleaner and more stable power supply.

This paper employs the PQ theory for calculating reference currents and utilizes hysteresis current controllers HCC for pulse signal generation to control the switching device of the SAPF. Moreover, the research introduces a parallel-operating Shunt Active Power Filter (SAPF) aimed at mitigating high-order harmonic currents within the load, significantly enhancing power quality while diminishing disruptions caused by harmonic distortions. The prevalence of nonlinear loads in industrial, commercial, and residential systems has precipitated substantial power quality challenges in modern power distribution systems. Notably, harmonic currents and reactive power emerge as pivotal concerns among these issues.

The paper's structure is delineated as follows: Section 2 provides a brief description of the CFL load used and presents the experimental impact of the massive use of these loads on the power system. Section 3 intricately details the three-phase four-wire Shunt Hybrid Power Filter SHPF with a four-leg configuration and split capacitor topology. This section also offers insights into the design and modeling of Passive Filter. Also, it provides a detailed analysis of the application of the PQ theory for calculating compensation current and the Fixed

Hysteresis Control method implemented to manage the switching devices of the APF. Furthermore, Section 4 presents an exhaustive analysis of simulation results and the effectiveness of harmonic mitigation strategies. Finally, Section 5 concludes the paper by summarizing the findings and contributions of this research pursuit.

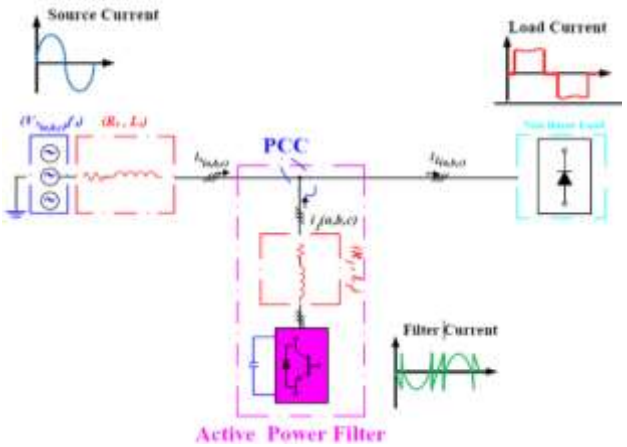

Fig. 1: Bloc diagram of the SAPF connected to the distribution network

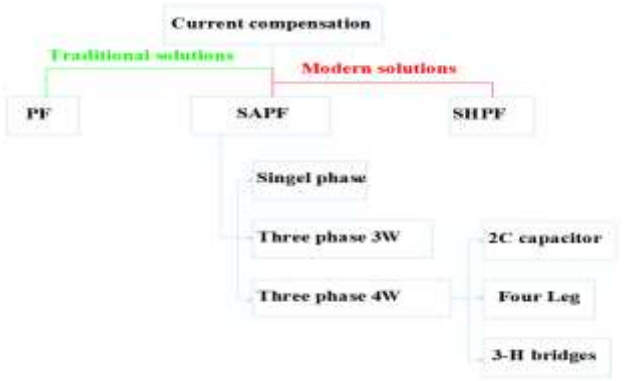

Fig. 2: Harmonic current compensation classification based on the power circuit

2 Investigation of the Impact of CFL Loads based on Experimental Tests

To quantify the effect of the massive use of CFL loads on the distribution network many experimental previous tests were carried out, [13]. Figure 3 shows the general scheme proposed in the experimental setup for a large number of GE CFL lamps powered by a three-phase system, this figure includes 75 lamps distributed across 3 AC-50Hz phases (25 lamps in parallel for each phase). A power analyzer, C. A 8336, is used to obtain data related to electrical parameters for any given point. The analyzer is configured in three-phase mode. This device is used to visualize data on-site and store it in digital form, which can be later retrieved using a computer and software provided by the manufacturer of the power analyzer. Therefore, it is important to note that all experimental figures in this research work are generated using the software provided by the manufacturing company (the latest version), called "Power Pad III" designed for all Chauvin Arnoux CA 8331, 8335, and 8336 devices, [14].

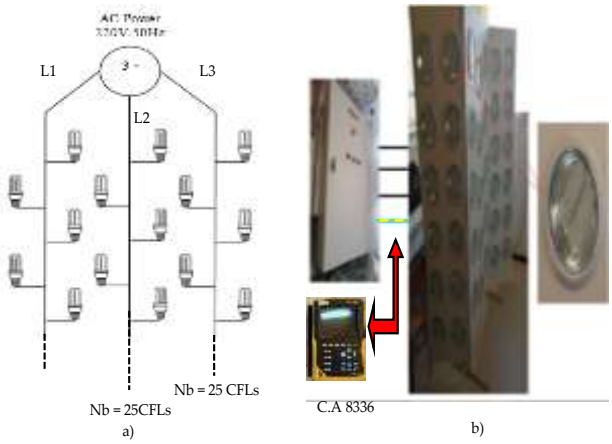

Fig. 3: Experimental setup for harmonic CFL investigations

Chauvin Arnoux CA 8331, 8335, and 8336 devices, [15], utilize equation (1) to compute the various harmonics (X_{THD}) for both voltage and current. Additionally, equation (2) is employed to determine the corresponding angle (φ_k) in degrees (°) relative to the fundamental. It is important to highlight that these calculations are executed through a 16-bit FFT with 1024 data points covering four cycles, and a rectangular window is applied following the specifications outlined in IEC61000-4-7. The harmonic factor for each phase (j) and order (h) is then derived from the real parts (b_k) and imaginary parts (a_k) expressed in equation (3).

$$X_{THD}[j] = \frac{\sqrt{\sum_{h=2}^{50} X[j][h]^2}}{X[j][1]} \quad (1)$$

$$\varphi_k = arctan\left(\frac{a_k}{b_k}\right) - \varphi_4 \quad (2)$$

where, X denotes the signal captured by the device, representing either the current (A) or the voltage (V) of the load. $X[j][1]$ specifically signifies the fundamental signal for each phase j (where $1 \leq j \leq 3$), and the variable h corresponds to the harmonic index.

$$\begin{cases} a_k = \frac{1}{512}\sum_{S=0}^{1024} F_s \cos(\frac{k\pi}{512}s + \varphi_k) \\ b_k = \frac{1}{512}\sum_{S=0}^{1024} F_s \sin(\frac{k\pi}{512}s + \varphi_k) \end{cases} \quad (3)$$

In this context, F_s represents the sampled signal at the fundamental frequency f_4, and k stands for the index of the spectral spike. It's essential to note that the order of the harmonic component is directly related to $k/4$.

From the founded results in [13], it is easy to observe that the current waveforms of CFLs are not sinusoidal for all three phases and are not in phase with the source voltages. Also, the neutral current is not equal to zero. The harmonic spectrum of CFLs, summarizes the origins of these disturbances and the non-linearity of the load. This load acts as a generator of significant harmonic currents that propagate back to the distribution source, potentially affecting other loads connected to the same network. Various parameters measured by the power analyzer are illustrated in Table 1.

Table 1. Main measured parameters with C.A 8336

P (kW)			***PF***		
Phase « a »	***Phase « b »***	***Phase « c »***	***Phase « a »***	***Phase « b »***	***Phase « c »***
0.5013	*0.5013*	*0.4943*	*0.668*	*0.655*	*0.647*
S (kVA)			***$I_{\_rms}$ (A)***		
Phase « a »	***Phase « b »***	***Phase « c »***	***Phase « a »***	***Phase « b »***	***Phase « c »***
0.7507	*0.7793*	*0.7636*	*3.16*	*3.27*	*3.2*
$V_{\_rms}$ (V)			***φ (°)***		
Phase « a »	***Phase « b »***	***Phase « c »***	***Phase « a »***	***Phase « b »***	***Phase « c »***
237.5	*238.1*	*237.4*	*24*	*24*	*24*
A_{THD} (%)			***V_{THD} (%)***		
Phase « a »	***Phase « b »***	***Phase « c »***	***Phase « a »***	***Phase « b »***	***Phase « c »***
86.2	*88.5*	*90.4*	*5.4*	*5.3*	*5.3*

For instance, the total powers absorbed by 75 GE LFC 20W lamps distributed across phases a, b, and c are respectively *P(a) = 501.3W*, *P(b) = 501.3W*, and *P(c) = 494.3W*. Additionally, poor power factors of *0.668*, *0.665*, and *0.647* are observed for the three phases. Despite the low active power consumed by these CFLs, the reactive power consumed is significantly considerable for phases a, b, and c, with *S(a) = 0.7507 kVA, S(b) = 0.7793 kVA, and S(c) = 0.7636 kVA*.

Figure 4 presents the experimental results of the effect of harmonic distortion of voltages as a function of the number of lamps for phase a. Also, as depicted in Table 1 and Figure 4, an increase in voltage THD $V_{\_THD}$ from *3.4%* to *5.3%*. This value is outside the order of the international standards, [11], [12]. It provides a detailed measurement for the three-line source. For instance, the $A_{\_THD}$ for the three phases a, b and c are *86.2%, 88.5%*, and *90.4%,* respectively. From Table 1 it can be also seen that the CFL current was delayed to the voltage of *24°* for the three phases, which may have harmful effects on the distribution network.

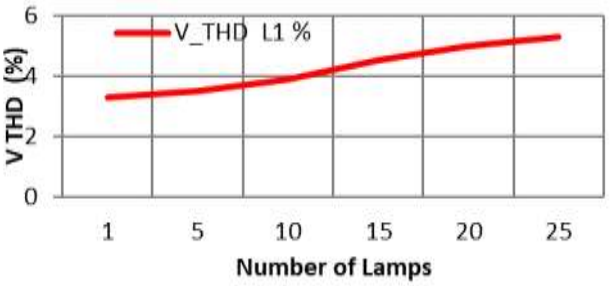

Fig. 4: Voltage THD as a function of the number of lamps (Experimental setup)

To improve the power quality and to cancel the harmonics generated by these non-linear loads on the mains side, we will present in the next two sections the proposed filter. At first, a passive power filter for some special harmonic currents ranks compensations applied for the same load. Second, an active power filter will be applied to attenuate all other harmonics and for reactive current compensation. Both filters are connected in parallel with the load.

3 Shunt Hybrid Power Filter

When both voltage and current are causing problems and distortion in the power system, more sophisticated filters are employed. These filters, known as hybrid filters, [16], are a combination of active and passive filters. Designing a passive filter necessitates a thorough understanding of the harmonic-producing load and the power system. Passive filters, because they always provide reactive compensation to a certain extent depending on the volt-ampere rating and voltage of the capacitor bank used, can be designed to serve the dual purpose of filtering and power factor correction to the desired level, [17]. As a result, passive filter design must consider potential increases in harmonic current sources or load reconfiguration, as these factors can lead to overloading, which can develop quickly.

3.1 Passive Filter

Passive filters are electrical devices that reduce the propagation of harmonics produced by non-linear

loads. A passive filter is installed in parallel to the power grid as shown in Figure 5, providing a very low impedance around the frequency to be filtered. Two types of passive filters can be distinguished: the resonant passive filter, and the damped passive filter or high-pass filter, [18]. They are presented respectively, by Figure 6(a) and Figure 6(b) The primary components of a passive filter include inductance *L*, capacitance *C*, and resistance *R*. Compared to other harmonic elimination methods; passive filters are relatively inexpensive. Their applications include shunting harmonic currents away from the power line or blocking their flow between system components by tuning the elements to resonate at a selected harmonic frequency, [19].

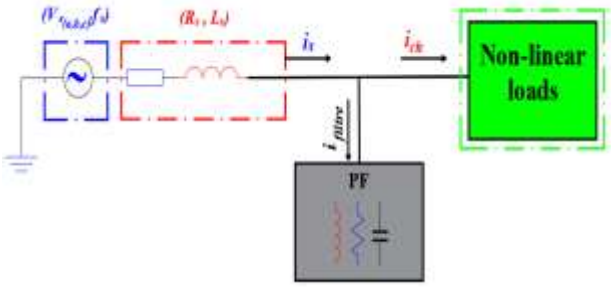

Fig. 5: Basic single-line diagram of a passive compensator

a) Resonant passive filter b) Damped passive filter

Fig. 6: Types of Passive Filter

- **Resonant passive filter:** It is a very selective filter. It can be connected in parallel with other resonant filters.
- **Damped passive filter:** It is the preferred choice for attenuating a whole frequency band.

These devices are used to prevent harmonic currents from propagating in electrical grids. They can also be used to compensate for reactive power. Despite their widespread use in industry due to their ease of installation, these devices can present many disadvantages, such as their short lifespan and very little flexibility;

- Lack of flexibility to adapt to network and load variations.
- Bulky equipment.
- Resonance problems with network impedance.

The presence of multiple harmonic orders, including the 3rd, 5th, 7th, and 11th, in the measured current necessitates the implementation of harmonic filtering. Two filter configurations are viable options: a single second-order, C-type high-pass filter or a combination of parallel-connected single-tuned filters. A comprehensive analysis conducted in [20], revealed that employing a set of combined single-tuned filters, each tuned to the respective 5th, 7th, and 11th harmonic orders, is the most effective strategy for mitigating these three harmonic orders. In contrast, a second-order high-pass filter is utilized to address harmonics ranging from the 17th to the 49th orders.

3.2 Passive Filter Design Parameters

In a three-phase system with loads like compact fluorescent lamps, the utilization of parallel passive filters proves to be a critical solution for mitigating harmonic distortions. These filters are designed to control specific harmonics generated by these non-linear loads, thus significantly improving the power quality. Mathematically, the design of these parallel passive filters involves the use of fundamental equations based on the passive filter topology.

3.2.1 Single-tuned (Resonant) Filter Design

For instance, in a parallel RLC filter, the filter impedance can be determined by equation (4), [21].

$$Z(\omega) = \frac{1 - LC\omega^2 + jRC\omega}{jC\omega} \tag{4}$$

where *Z* represents the impedance, *j* is the imaginary unit, ω is the frequency, *C* is the capacitance of the capacitor, and *L* denotes the coil's inductance. These filters selectively divert undesirable harmonics to enhance current quality and ensure a more stable operation of the three-phase electrical system.

The sizing of the different parameters *R*, *L*, and *C* is done by the following equations (5)-(9)

$$C = \frac{Q_c}{2\pi f V^2} \tag{5}$$

$$X = \frac{1}{2\pi f h C} = \sqrt{\frac{L}{C}} \tag{6}$$

$$L = \frac{X}{2hf} \quad (7)$$

$$Q = \frac{2\pi fL}{R} \quad (8)$$

$$R = \frac{1}{2\pi fC} \quad (9)$$

In this context, X represents the reactance of either the inductor or the capacitor at the resonant frequency. Also, it should be noted that a typical range for Q must be between 30 and 60.

3.2.2 Single Tuned (Resonant) Filter Design

The second-order high-pass filter resembles a single-tuned filter, with the key difference being the parallel arrangement of inductors (L) and resistors (R) instead of the series arrangement observed in single-tuned filters (Figure 6(b)). This configuration offers enhanced filtering performance and reduces energy losses at the fundamental frequency.

The impedance of this filter is given by equation 10:

$$Z(\omega) = \left(\frac{1}{R} + \frac{1}{j\omega L}\right)^{-1} + \frac{1}{j\omega C_1} \quad (10)$$

But the quality factor is different compared to the single tuned filter, it is given by 11:

$$Q = \frac{R}{\sqrt{\frac{L}{C}}} = \frac{R}{X_{LN}} = \frac{R}{X_{CN}} \quad (11)$$

3.3 Shunt Active Power Filter

The active filter connected in parallel to the network, as shown in Figure 1, [22], [23], is most often controlled as a current generator. It injects into the network disruptive currents equal to those absorbed by the polluting load but in phase opposition with them, in order to restore the electric network current to a sinusoidal shape, as illustrated in Figure 7(c). It prevents disruptive currents (harmonics, reactive, and unbalanced currents) produced by polluting loads from flowing through the impedance of the network, located upstream of the active filter connection point. Figure 1 represents the general structure of the parallel active filter, which consists of a single block. Only the power parts were presented. The control-command part will be presented in the next section. The power part is composed of the:

1. A voltage inverter based on power switches, controllable at initiation and blocking (GTO, IGBT, etc.) with anti-parallel diodes.
2. An energy storage circuit, often capacitive.
3. An output filter.

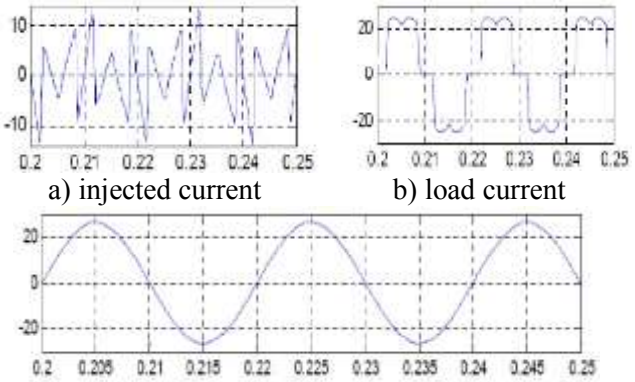

a) injected current b) load current

c) Source current

Fig. 7: Source current at different points of APF applied to a 3 phases rectifier connected to an RL load

3.3.1 Mathematical Fundamentals of the Harmonic Detection Technique

The load current is influenced by the line impedance connected to the power sources during steady-state conditions and the equations for calculating the load current can be derived as follows, [24]:

$$i_{L_{(a,b,c)}}(t) = i_{p_{(a,b,c)}}(t) + i_{q_{(a,b,c)}}(t) + i_{h_{(a,b,c)}}(t) \quad (12)$$

Where :

$$i_{p_{(a,b,c)}}(t) = i_1 \cos(\varphi_1),$$

$$i_{q_{(a,b,c)}}(t) = i_1 \sin(\varphi_1), \text{ and}$$

$$i_{h_{(a,b,c)}}(t) = i_3\sqrt{2}\sin(3\omega t + \varphi_3\frac{\pi}{180}) + \sum_{h=5}^{49} i_h\sqrt{2}\sin(h\omega t + \varphi_h\frac{\pi}{180})$$

It is clear from equation (12) that the variables $i_{p_{(a,b,c)}}(t)$, $i_{q_{(a,b,c)}}(t)$ and $i_{h_{(a,b,c)}}(t)$ represent the fundamental active current, fundamental reactive current, and the harmonic current of the Three-Phases Four-wires load respectively. To compensate the harmonic and reactive currents, the active current can be isolated from the equation. Thus, the required compensation currents (13) that the active power filter must generate are those that need to be injected.

$$i_{compensation}(t) = i_{f(a,b,c)}(t) = -i_{q(a,b,c)}(t) + i_{h(a,b,c)}(t) \quad (13)$$

The overall efficiency of the Active Power Filter (APF) was discovered to hinge on both the accuracy of the reference current extraction method and the control of Voltage Source Inverter (VSI) switching devices. To extract reference currents, an algorithm rooted in the PQ technique was devised and implemented. This algorithm facilitated the real-time extraction of harmonics produced by Compact Fluorescent Lamps (CFLs) from the power source. These extracted currents were sensed through four strategically placed sensors on the load side. The compensation currents were then compared to the actual currents supplied by the VSI at the Point of Common Coupling (PCC). Any disparities detected were treated as error currents and employed in the Fixed Hysteresis Control Algorithm (HCA) to generate switching signals for the VSI via Insulated Gate Bipolar Transistor (IGBT) switches.

3.3.2 Algorithm for Current Identification

Typically, the primary function of a Shunt Active Power Filter (SAPF) involves filtering or compensating for disturbances (harmonic, reactive, unbalanced, etc.) originating from both linear and non-linear loads on the electrical grid. The identification method serves to calculate perturbing currents that the Voltage Source Inverter (VSI) will inject, via the output filter, into the Point of Common Coupling (PCC) in a phase opposite to the disturbance. Consequently, the electrical grid side is maintained in a clean state, exhibiting sinusoidal current and voltage patterns.

3.3.3 Review of the Instantaneous Reactive Power Theory (PQ Theory)

The prevailing identification method, widely adopted, is the instantaneous real and imaginary powers approach, [3]. This technique presents the benefit of simultaneously and precisely compensating for harmonic currents, unbalanced currents, and reactive power, either partially or selectively. It achieves this accuracy swiftly and with ease. It was implemented in 1983, [25]. They introduced the "Generalized Theory of the Instantaneous Reactive Power in Three-Phase Circuits," commonly known as the instantaneous power theory or PQ theory. This theory is based on instantaneous values in three-phase power systems with or without neutral wire, and can be applied to steady-state or transitory operations with various voltage and current waveforms. The PQ theory involves transforming the three-phase voltages and currents in the (a-b-c) coordinates to the (α-β-0) coordinates using the Clarke transformation as presented in equations (14) and (15), and then calculating the PQ theory instantaneous power components, [26].

The PQ theory's advantage is that it separates the zero sequence components which do not contribute to the alpha and beta components. Therefore, it can be neglected in a balanced system. Figure 8 represents the block diagram of the proposed methodology.

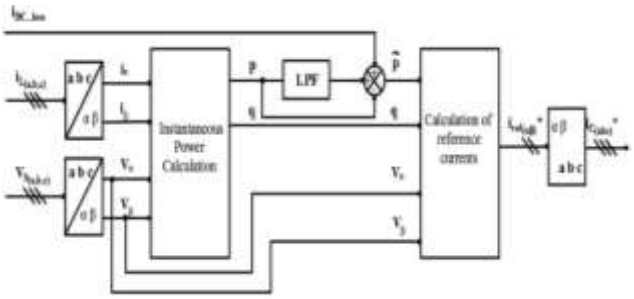

Fig. 8: Block diagram of the PQ theory

$$\begin{pmatrix} i_\alpha \\ i_\beta \\ i_0 \end{pmatrix} = \sqrt{\frac{2}{3}} \begin{pmatrix} 1 & \frac{1}{2} & \frac{1}{2} \\ 0 & \frac{\sqrt{3}}{2} & \frac{\sqrt{3}}{2} \\ \frac{1}{\sqrt{2}} & \frac{1}{\sqrt{2}} & \frac{1}{\sqrt{2}} \end{pmatrix} \begin{pmatrix} i_a \\ i_b \\ i_c \end{pmatrix} \quad (14)$$

$$\begin{pmatrix} V_\alpha \\ V_\beta \\ V_0 \end{pmatrix} = \sqrt{\frac{2}{3}} \begin{pmatrix} 1 & \frac{1}{2} & \frac{1}{2} \\ 0 & \frac{\sqrt{3}}{2} & \frac{\sqrt{3}}{2} \\ \frac{1}{\sqrt{2}} & \frac{1}{\sqrt{2}} & \frac{1}{\sqrt{2}} \end{pmatrix} \begin{pmatrix} V_a \\ V_b \\ V_c \end{pmatrix} \quad (15)$$

The power components p and q are related to the same α-β voltages and currents and can be written together:

$$\begin{bmatrix} p \\ q \end{bmatrix} = \begin{bmatrix} V_\alpha & V_\beta \\ V_\beta & -V_\alpha \end{bmatrix} \cdot \begin{bmatrix} i_\alpha \\ i_\beta \end{bmatrix} \quad (16)$$

Where $p_0 = v_0 \cdot i_0$ instantaneous zero-sequence power. The harmonics component can be eliminated by using a Low Pass Filter (LPF). After selecting and eliminating the harmonic current, it is necessary to apply the inverse of Clarke transformation (Equation 17) to calculate the reference current in the (a,b,c) frame.

$$i_{c_{(a,b,c)}}{}^* = \begin{pmatrix} i_{c_a}{}^* \\ i_{c_b}{}^* \\ i_{c_c}{}^* \end{pmatrix} = \sqrt{\frac{2}{3}} \begin{pmatrix} \frac{1}{\sqrt{2}} & 1 & 0 \\ \frac{1}{2} & -1 & \frac{\sqrt{3}}{2} \\ \frac{1}{\sqrt{2}} & \frac{1}{2} & \frac{\sqrt{3}}{2} \end{pmatrix} \begin{pmatrix} i_{c_\alpha} \\ i_{c_\beta} \\ i_{c_0} \end{pmatrix} \quad (17)$$

3.3.4 Advantage of the PQ theory in SAPF

The control of active filters can be achieved using various methods, including the p-q theory. The p-q theory has notable advantages such as being inherently designed for three-phase systems, regardless of their balance or unbalance, with or without harmonic distortions in both voltages and currents. Additionally, it relies on instantaneous values, enabling a high level of dynamic response. Furthermore, its computations are relatively straightforward, utilizing only algebraic expressions that can be implemented using standard processors. Lastly, it offers two control strategies, namely constant instantaneous supply power and sinusoidal supply current. It is applicable for all industrial and residential loads applications.

3.3.5 Conventional Fixed Hysteresis Band

The conventional hysteresis fixed band technique employs two bands, namely the upper band and the lower band represented by Δ+ and Δ-, respectively. The modulated current is confined between these two bands. When the error current ε_a approaches the upper band Δ+, the upper IGBT switch F_a, is switched off while the lower switch $\overline{F_a}$ is switched on, and vice versa for the lower band Δ-. This ensures that the compensating current $i_{c(a,b,c)}*$ tracks the reference current $i_{r(a,b,c)}$, this achieving robustness and good dynamic performance compared to other compensation methods. Figure 9(a) and Figure 9(b) illustrate the block diagram of the conventional hysteresis control and the waveform of the control signals for a single phase (phase a). It is to be noted that the lower side of the inverter is controlled by the same signal but with a NOT logic gate.

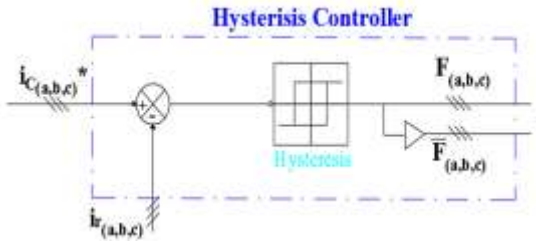

a)

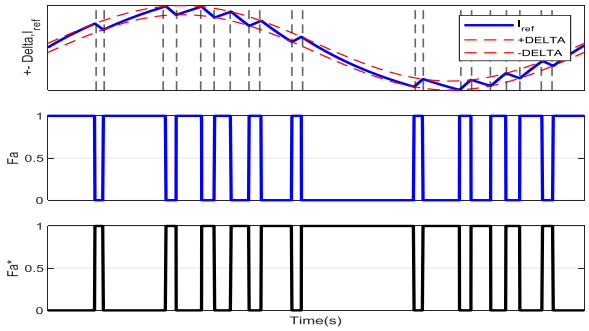

b)

Fig. 9: Block diagram of the constant hysteresis modulation and their principle of generating control signals

The fixed hysteresis band has certain advantages, such as:

- **Simplicity:** A fixed hysteresis band is relatively simple to implement because it does not require additional components such as sensors or microcontrollers.
- **Quick Response:** it can allow a quick response of the filter in case of variation of load or source conditions, which can improve the quality of the output signal.
- **Low distortion:** it can reduce signal distortion by limiting variations in filter resonance frequency.
- **Low cost:** Fixed hysteresis band does not require expensive components, which can reduce the cost of manufacturing the filter.

However, it is important to note that these benefits may vary depending on filter specifications and operating conditions. Also, while this method has some advantages, it has several disadvantages, including:

- **Limited range Frequency:** The fixed hysteresis band is suitable for a limited frequency range. If the source frequency exceeds this range, the filter may not function properly, which may cause signal distortion.
- **Sensitivity to temperature variations:** The properties of the electronic components that make up the filter can vary with temperature changes. This can result in the drift of resonant frequencies and affect the accuracy of the fixed hysteresis band.
- **Non-linear effects:** The fixed hysteresis band can also produce non-linear effects that can alter the waveform of the output signal. These non-linear effects may be due to interactions between filter components or saturation of the feedback circuit.

As presented previously to improve the performance, and mitigate the disadvantages mentioned below we can use a PWM controller instead of an HCC. But this is not the subject of this paper.

3.4 Filters Selection

From previous experimental research carried out to investigate the effect of harmonics generated by CLFs at the side of the main. We can notice that at lower harmonic frequencies, most waveforms have a high percentage of harmonic distortion compared to the harmonic frequency. Hence CFLs are characterized by the high harmonic emission for low and high harmonic order frequency, therefore, a 2nd-order high-pass filter is used to remove the higher-order frequencies injected by CFL and by the switched device of the APF, as shown in Figure 10. So, that's why in this research we interest only for the 2nd order high-pass filter filters for high harmonic current 21th to 49th) and the other harmonics will be mitigated by the SAPF.

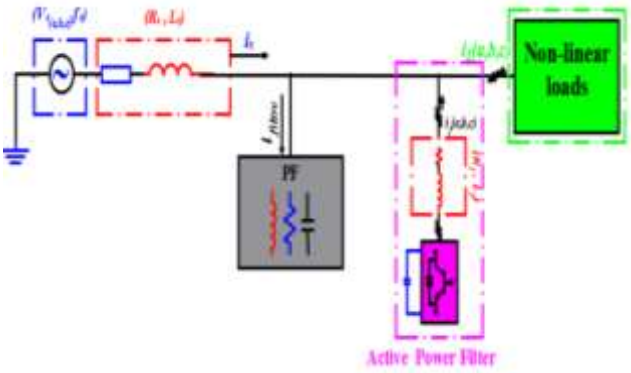

Fig. 10: Basic single-line diagram of a hybrid active power filter topology based on a passive filter in parallel with an active power filter

4 Simulations and Results

The studied shunt hybrid system is simulated using Matlab/Simulink software, by using the Simscape power system library toolbox. The load is constituted of 75 equivalent models of 20W lamps distributed over the 3 AC phases. A passive filter is connected in parallel to attenuate the high harmonic rank (from harmonic 21st). Also, a three-phase four-wire SAPF with three legs and the ford leg connected to a split capacitor (2C topologies) is connected in parallel with the load. Table 2 summarizes the simulation parameters. The circuit diagram of the full part of the HAPF is presented in Figure 11. The passive filter is connected at *t=0.04s*, and the HAPF is connected to PCC at time instant *t = 0.08* seconds.

Table 2. Power System Parameters.

Parameters		Symbol	Values
Grid	System frequency	*Fs*	50 HZ
	Source voltage	*Vrms*	230V
	Source resistance	*Rs*	2mΩ
	Source inductance	*Ls*	1mH
Passive filter	PF capacitance	C_{PF}	nF, µF
	PF inductance	L_{PF}	mH
	PF resistance	R_{PF}	4.7Ω
Shunt active power filter SAPF	Filter resistance	*Rf*	1mΩ
	Filter inductance	*Lf*	0.1µH
	DC side capacitance	C_1, C_2	2200µF
	Reference voltage	*Vdc*	600V

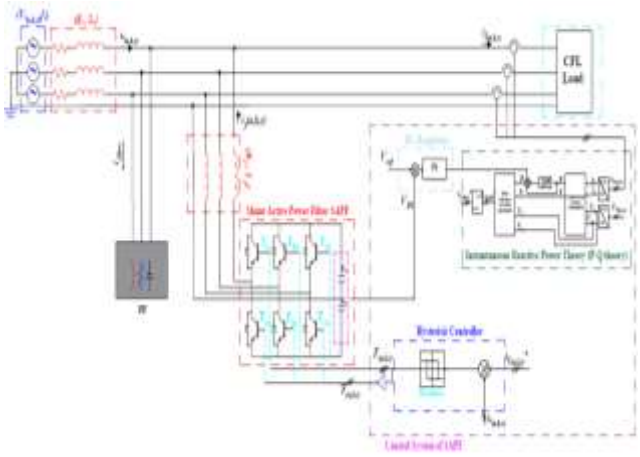

Fig. 11: Circuit diagram of a three-phase four-wire HAPF with PQ and Hysteresis Controller

Where $I_{L_{(a,b,c)}}$, $I_{C_{(a,b,c)}}$, $I_{S_{(a,b,c)}}$ and $V_{S_{(a,b,c)}}$ are the load currents before compensation, the compensating current injected by the power device (the SAPF), the source currents after compensation, and the source voltage, respectively.

4.1 Simulation Result before Compensation

The simulated results of the source voltage $V_{S_{(a,b,c)}}$ and currents waveforms $I_{L_{(a,b,c)}}$ before connecting the PF and the APF to the system the three-line

system are presented in Figure 12(a) and Figure 12(b), respectively.

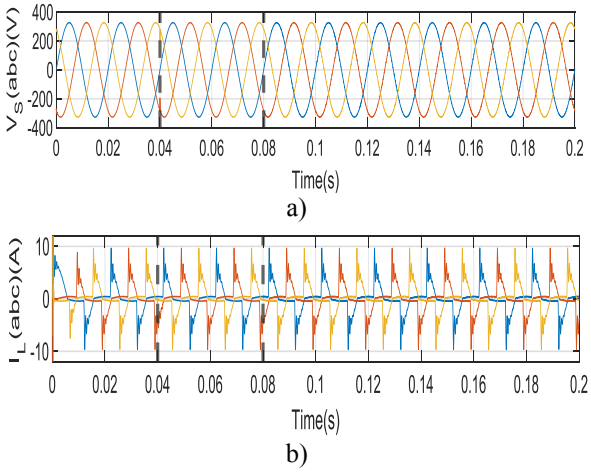

Fig. 12: Source voltage and current waveforms before compensation

The current waveforms generated by CFLs deviate from sinusoidal shapes across all three phases and are not synchronized with the source voltages. Furthermore, the neutral current is different to zero. The harmonic spectrum of CFLs presented in Figure 13 serves to encapsulate the sources of these disruptions, highlighting the non-linear behavior of the load. Essentially, this load functions as a generator of notable harmonic currents with $A_{THD} = 90.75\%$, which have the potential to propagate back to the distribution source, thereby impacting other loads connected to the same network. Also, it should be noted that all simulated parameters are almost identical to the experimental simulation carried out in [13]. Wish means that the current waveforms of the real model and the simulation model reproduce the same waveforms and also the same FFT components.

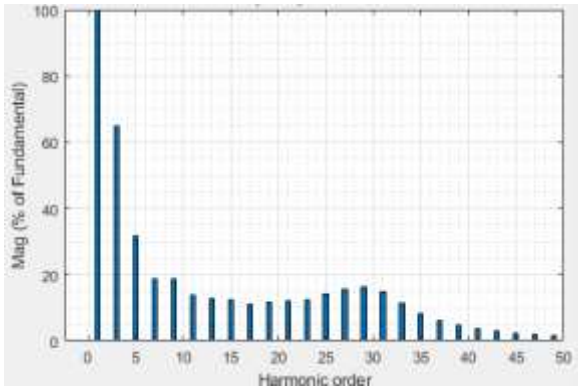

Fig. 13: FFT components of the load current before compensation

4.2 Performance of the Passive Filter

The passive filter is suggested for its simplicity, cost-effectiveness, and dependable performance. Utilizing system parameters and measured harmonics. A 2nd order high-pass filter is used to remove the higher-order frequencies injected by CFLs and by the switched devices of the APF. After connecting the PF at t=0.04s we can notice that the THD is reduced from 90.75% to 71.22% (as presented in Table 3); which means that the PF is well designed for attenuated those high harmonic orders frequency. However, the power quality still contains the low harmonic frequency and noise, and the full system is still outside the national and international standards, [11], [12]. So, a force needs an SAPF to attenuate others' harmonic rank. Wish is implemented in the next section to make the source current and voltage align with predefined international standards.

Table 3. THD Percentage Comparison

THD without PF Filters	THD with PF Filter
90.75%	71.22%

Figure 14(a) and Figure 14(b), represent respectively, the current waveforms of the compensations current and the source current before and after connecting the APF to the system at t=0.08. Also, Figure 15 represents the source current FFT after connecting the SHPF.

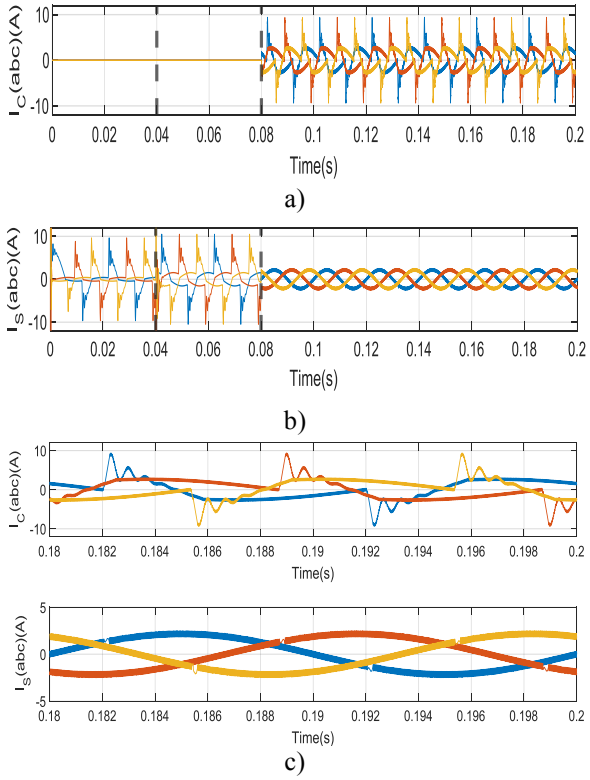

Fig. 14: Current waveforms before and after compensation at different points

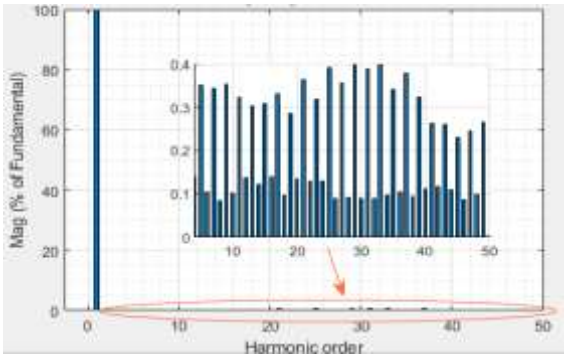

a)

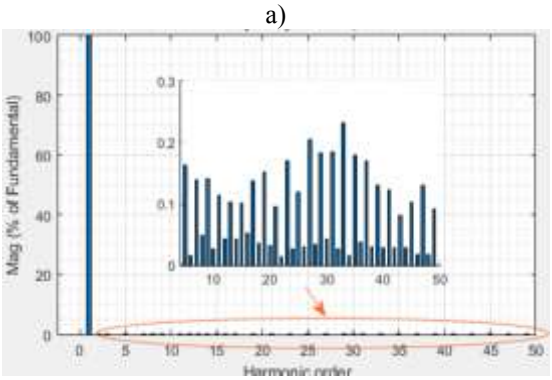

b)

Fig. 15: FFT components of the source current after compensation (a) with APF, and (b) with HAPF

As shown in Figure 15(a) and Figure 14(a) represent the FFT component and the current waveforms of the CFLs before connecting the SAPF, it can be noticed that the THD of the current $A_{THD} = 90.75\%$, and the THD of the voltage $V_{THD} = 5.3\%$. Moreover, Figure 14(a) and Figure 14(c) show that the system corresponds to a poor factor due to the phase shift between the current and voltage. According to the international, [11], [12], standards, these results are outside of the allowed limits and can cause harmful effects on the distribution network. As result of this work, and after connecting the SHPF at *t=0.06s* to the system, it is clear from Figure 14(b) and Figure 14(c) that the currents waveforms of the source $I_{S_{(a,b,c)}}$, become almost sinusoidal, which attests that the conventional algorithm used in this paper has succeeded in compensating harmonic currents; by injecting equal but opposite harmonic current to the power network. In addition, the source currents and voltage are in phase as presented in the same figure, which results in obtaining a good power factor PF close to 1. Figure 15(a) shows that the THD of the current A_{THD} after compensation becomes equal to 1.75%, (a good reduction in THD is noticed) with a APF and to 0.75% with a HAPF (Figure 15(b)). Also, the fundamental current values for phase "a" remain almost the same before and after connecting the HAPF to the system where $I_{S\_Bef\_1a} = 3.19A$ and $I_{S\_Aft\_1a} = 3.23A$. This implies that the filter injects only harmonic currents, while the network injects only the fundamental component of the load current.

4.3 Performance under Different Scenarios

To investigate and validate the performance of conventional algorithms and the fixed hysteresis controller, two distinct case studies have been undertaken. This could involve essentially sudden changes in the load part. Variations in source voltage, or other external factors that might affect system performance will be the case of another future research anyways, these cases are outlined as follows:

Case 1: Variable and Balanced Load of 100% CFLs: In this scenario, a load of 99 Compact Fluorescent Lamps (CFLs), with 33 lamps connected per phase, is employed from t0=0s to t2=0.14s. Subsequently, at t2=0.14s, the load is doubled to 150 lamps, maintaining a balanced distribution across the three phases.

Case 2: Unbalanced Load: This case involves an unbalanced load configuration, with 75 lamps for Phase A, 100 lamps for Phase B, and 120 lamps for phase c.

Figure 16 and Figure 17 depict the current waveforms of the Shunt Active Power Filter (SAPF) both before and after compensation for Case 1 and Case 2. Notably, the SAPF is activated at t1=0.04s for Case 1, while Case 2 retains the same configuration as previously established in the study. These visual representations provide insights into the SAPF's effectiveness in mitigating power quality issues under varying load conditions, showcasing its performance in both balanced and unbalanced load scenarios.

Figure 16 displays simulation results with a variable load of 100% CFLs. The SAPF effectively adjusts to load variations, maintaining sinusoidal source currents throughout load changes. The Total Harmonic Distortion (THD) of the source decreases from 89.66% to 2.18% with the connection of 99 lamps (from t1=0.04s to t2=0.14) and from 92.2% to 2.44% with 150 lamps connected (at t2=0.14s). The fundamental currents for these configurations are 2.8A and 5.2A, respectively. Note that t0, t1, and t2 are arbitrarily chosen for this study.

In Figure 17, the SAPF response to an unbalanced load (75 lamps for Phase A, 100 lamps for Phase B, and 120 lamps for Phase C) is presented. Although the source currents are sinusoidal for each phase, they are unfortunately not balanced with the simple hysteresis controller. However, the THD is reduced from 89% to 2.56% for Phase A, 90.3% to 2.67% for Phase B, and 90.9% to 2.7% for phase c. The fundamental currents for the three phases are 2.4 A, 2.6 A, and 2.8 A, respectively.

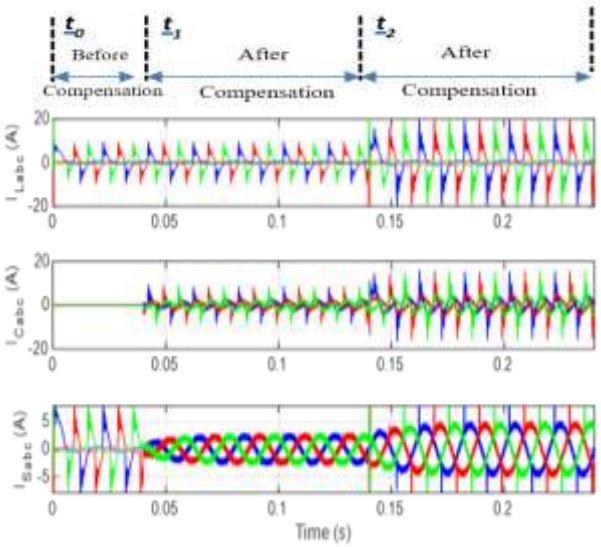

Fig. 16: Current waveforms before and after compensation under case 1

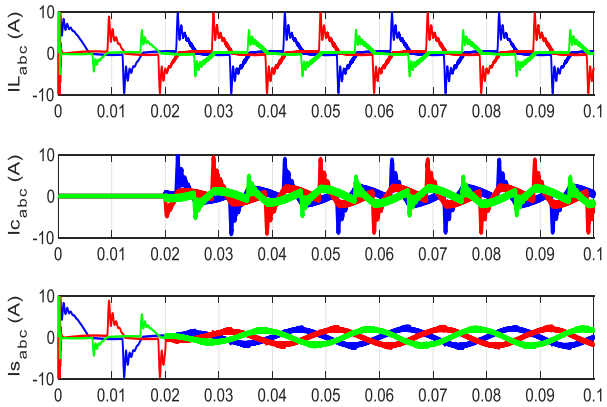

Fig. 17: Current waveforms before and after compensation under case 2

4.4 Performance under Different SAPF Topologies:

In this section, we present the performance of the shunt active power filter with three phase four wire different active power filter topologies, respectively, with the four legs topologies. With the four legs and mid-point capacitor topologies and with 3 half-bridge topologies presented in Figure 18(a), Figure 18(b) and Figure 18(c). These SAPF configurations are widely employed to address power quality issues in the grid or distribution medium, particularly in higher power applications. Moreover, these topologies can effectively mitigate issues related to the duty cycle *dv/dt* of active switches. Nevertheless, the primary drawbacks of these configurations include a substantial number of switching devices, intricate control techniques, sizable physical dimensions, and elevated costs.

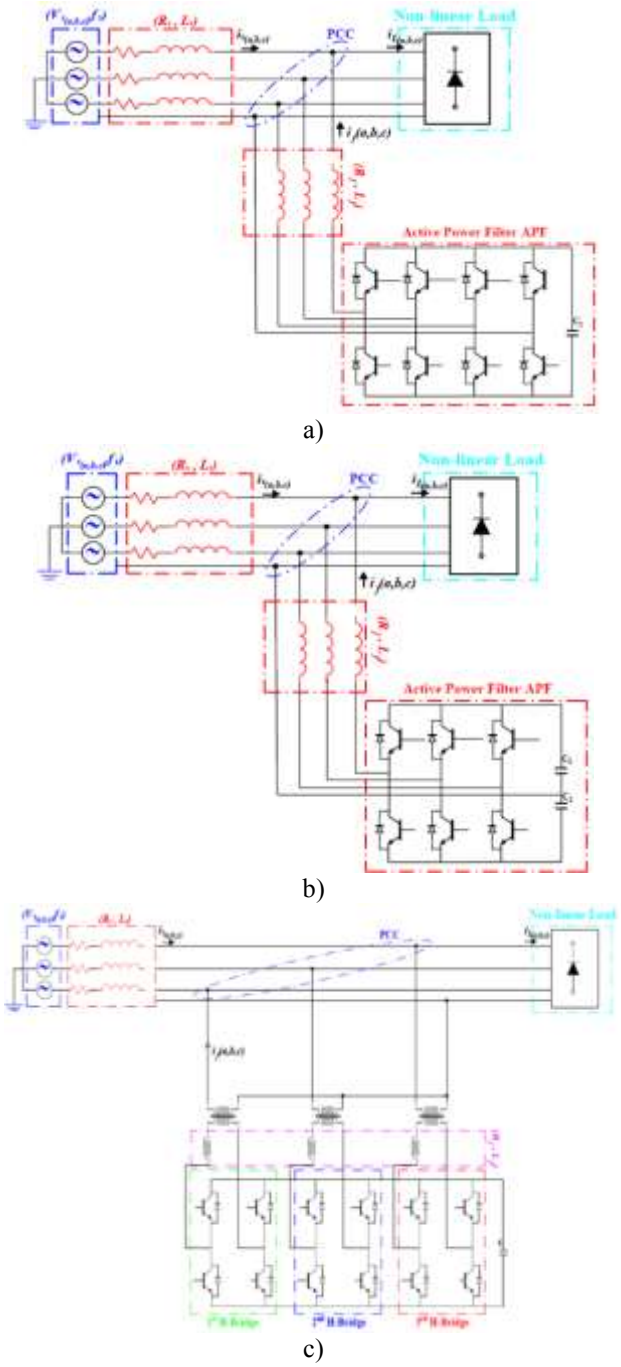

Fig. 18: Bloc diagram of the SAPF connected to distribution network a) with four legs topologies, b) with four legs and mid-point capacitor topologies, and c) with 3 half-bridge topologies

As known that The THD of the current before compensation of the load is equal to 90.75%. After connecting the SAPF with the 2C topology, the THD is reduced to 1.75%. With the four legs topologies the THD of the source current is improved to 1.25% and with the 3H bridge topology to 1%. However, the three applied topologies show their good application of filtering the harmonic currents generated by the non-linear load. Which implies that the network contains only the fundamental current.

SAPFs are used in power systems to mitigate harmonics and improve power quality. They are commonly employed in various industrial applications to address issues related to distorted power waveforms, reactive power, and harmonic currents. We can note some industrial applications of SAPFs such as Variable Frequency Drives, Industrial Automation and Robotics, Data Centers, Textile Industry, and Pharmaceutical and Chemical Industries. By installing SAPFs in these and other industrial and residential applications, companies can enhance power quality, reduce energy losses, and comply with regulatory standards related to harmonics and power factor correction.

4.5 Future Research

It's crucial to note that although the HCA method has numerous advantages, it is prone to chattering, resulting in inconsistent switching frequencies, which remained unresolved. To counter this issue, a Pulse Width Modulation (PWM) controller must be integrated into the system in place of HCA. This PWM controller served to stabilize the switching frequency and alleviate associated harmonic losses. Also, despite all the advantages of the SHPF, the DC bus of this filter uses a three-phase rectifier to provide the power energy to the capacitors to compensate for the reactive power generated by the nonlinear loads, which can create other problems of harmonics in case of highly non-linear loads. To overcome this issue, a hybrid active power filter HAPF powered up with a PV system to power the DC bus can be suggested for future work. Also, to further test the effectiveness and applicability of the suggested filter, different algorithms and scenarios including balanced and unbalanced nonlinear loads must be investigated and studied.

Finally, the integration of Computational Intelligence (CI) and Artificial Intelligence (AI) methods, such as Neural Networks, Fuzzy Logic, Petri Nets, and Evolutionary Computing, into the design of SAPF circuits in the context of PQ theory and hysteresis controller presents an intriguing avenue for enhancing performance and adaptability. CI techniques have demonstrated effectiveness in optimizing control strategies and mitigating power quality issues in various applications. For instance, neural networks have been employed for real-time learning and adaptation in power systems, [27], [28], while Petri nets and, fuzzy logic have shown their success in nonlinear system control and for multilevel inverter topology, they are offering robustness in dealing with uncertainties inherent in power electronics, [29], [30] and [31]. Evolutionary computing, on the other hand, has proven valuable in parameter tuning and optimization tasks in power systems. By leveraging these CI methodologies, the design of SAPF circuits could potentially benefit from improved efficiency, adaptability, and robustness, aligning with the current trends in power electronics research. So, it is recommended to use another intelligent control technique such as Petrie net algorithms, or neuronal algorithms for the current compensation calculation block. Wish is the work of future research. We will take into account the effect of the impedance of the cable even in simulation mode, [32].

5 Conclusion

The focus of this study is on power quality indices related to a residential power rectifier functioning as a nonlinear load. The analysis delves into harmonic distortions present in both the source current and voltage, considering both total and individual harmonic distortions. The measured values surpass the thresholds established by international standards for both current and voltage. To address and overcome this issue a SHPF based on a passive filter in parallel with an APF is designed and implemented. The APF is controlled with the PQ theory and a simple Hysteresis controller. Matlab simulation results validate the effectiveness of the proposed hybrid filter design, demonstrating an improvement in source current and voltage to meet the accepted levels specified by the international standard.

Beyond those traditional methods, the synergy between a hybrid active power filter powered up with a PV system offers a compelling avenue for harmonic mitigation, unlocking additional benefits that deserve dedicated exploration in future studies. Their control part will be suggested based on the current trend of Computational Intelligence such as Neural Networks, Fuzzy Logic, or Intelligence Artificial IA.

Nomenclature:

Notation	Description
CFL	Compact Fluorescent Lamp
PF	Passive Filter
APF	Active Power Filter
SAPF	Shunt Active Power Filter
HAPF	Hybrid Active Power Filter
VSI	Voltage Source Inverter
THD	Total Harmonic Distortion
PCC	Point of Common Coupling
HCA	Hysteresis control algorithms
FFT	Fast Fourier Transform
PFC	Power Factor Correction
PQ	PQ theory

References:

[1] İ. Kıyak, B. Oral, and V. Topuz, "Smart indoor LED lighting design powered by hybrid renewable energy systems," *Energy Build.*, vol. 148, pp. 342–347, 2017, doi: 10.1016/j.enbuild.2017.05.016.

[2] P. Verma, N. Patel, and N.-K. C. Nair, "Power quality impacts during CFL to LED transition," in *Australasian Universities Power Engineering Conference (AUPEC),Brisbane, QLD, Australia*, 2016, pp. 1-6. doi: 10.1109/aupec.2016.7749339.

[3] K. Naftahi, A. Abouloifa, Z. Hekss, S. Echalih, F. Ait Bellah, and I. Lachkar, "Three-Phase Four-Wire Shunt Active Power Filter Based on the Hybrid Automaton Control with Instantaneous Reactive Power Theory," *IFAC-PapersOnLine*, vol. 55, no. 12, pp. 532–537, 2022, doi: 10.1016/j.ifacol.2022.07.366.

[4] R. Arnold, "Solutions to the power quality problem," *Power Eng. J.*, vol. 15, no. 2, pp. 65–73, 2001, doi: 10.1049/pe:20010202.

[5] A. Chebabhi, M. K. Fellah, A. Kessal, and M. F. Benkhoris, "Comparative study of reference currents and DC bus voltage control for Three-Phase Four-Wire Four-Leg SAPF to compensate harmonics and reactive power with 3D SVM," *ISA Trans.*, vol. 57, pp. 360–372, 2015, doi: 10.1016/j.isatra.2015.01.011.

[6] B. Deffaf, H. Farid, H. Benbouhenni, S. Medjmadj, and N. Debdouche, "Synergetic control for three-level voltage source inverter-based shunt active power filter to improve power quality," *Energy Reports*, vol. 10, pp. 1013–1027, 2023, doi: 10.1016/j.egyr.2023.07.051.

[7] Z. Hekss, A. Abouloifa, I. Lachkar, F. Giri, S. Echalih, and J. M. Guerrero, "Nonlinear adaptive control design with average performance analysis for photovoltaic system based on half bridge shunt active power filter," *Int. J. Electr. Power Energy Syst.*, vol. 125, p. 106478, 2021, doi: 10.1016/j.ijepes.2020.106478.

[8] B. Nagi Reddy, A. Pandian, O. Chandra Sekhar, and M. Ramamoorty, "Performance and dynamic analysis of single switch AC-DC buck-boost buck converter," *Int. J. Innov. Technol. Explor. Eng.*, vol. 8, no. 4, pp. 307–313, 2019.

[9] Y. Ramachandra, M. Akhileshwar, A. Pandian, R. Nalli, and K. Subbarao, "Analysis of recent developments in brushless DC motors controlling techniques," *Int. J. Innov. Technol. Explor. Eng.*, vol. 8, no. 5, pp. 522–526, 2019.

[10] A. H. Fahad and M. S. Reza, "Single-Phase Shunt Active Power Filter Using Parabolic PWM for Current Control," in *Proceedings of the 7th International Conference on Smart Energy Grid Engineering, SEGE,Oshawa, ON, Canada, 2019*, 2019, pp. 134–138. doi: 10.1109/SEGE.2019.8859868.

[11] GENELEC, *Characteristics of the voltage supplied by public distribution networks "Caractéristiques de la tension fournie par les réseaux publics de distribution", EN 50 160, CLC/BTTF*, vol. 68. 1994, p. 6.

[12] S. Emv, A. G. Corporate, and H. Nordstrasse, "IEC 61000-3-2 Harmonics Standards Overview," *Schaffner EMC Inc., Edsion, NJ, USA*, pp. 1–5, 2005, [Online]. http://www.teseq.tw/pdfinfo/05_AN_IEC61000-3-25.pdf (Accessed Date: March 29, 2024).

[13] H. Mohamed, N. Mohamed, and S. Lassaad, "Experimental Investigations of a CFLs Currents Harmonics Injection into an Electrical Network Grid," in *2021 4th International Symposium on Advanced Electrical and Communication Technologies, ISAECT, Arabie Saoudi, 2021*, IEEE, 2021, pp. 1–5. doi: 10.1109/ISAECT53699.2021.9668434.

[14] Chauvin Arnoux, "Chauvin Arnoux software." [Online]. https://catalog.chauvin-arnoux.com/fr_en/c-a-8336.html?___from_store=fr_fr (Accessed Date: March 8, 2023).

[15] Chauvin Arnoux Manyfactory, "TECHNICAL DATA", [Online]. https://www.chauvin-arnoux.com/sites/default/files/HLHBXUP5.PDF (Accessed Date: March 8, 2023).

[16] R. Bahrekazemi, "Assessment of Different Compensation Strategies in Hybrid Active

Power Filters," *Int. J. Appl. Math. Comput. Sci. Syst. Eng.*, pp. 34–39, 2013.

[17] S. R. Reddy, P. V Prasad, and G. N. Srinivas, "Power Quality Improvement on 11kV/440V Distribution System using DSTATCOM," *Int. J. Electr. Eng. Comput. Sci.*, vol. 6, pp. 17–26, 2024.

[18] E. Kazemi-Robati and M. S. Sepasian, "Passive harmonic filter planning considering daily load variations and distribution system reconfiguration," *Electr. Power Syst. Res.*, vol. 166, pp. 125–135, 2019, doi: 10.1016/j.epsr.2018.09.019.

[19] M. M. Swamy, G. R. Bisel, and S. L. Rossiter, *"Passive harmonic filter system for variable frequency drives."* Google Patents, 1995.

[20] A. B. Nassif, W. Xu, and W. Freitas, "An investigation on the selection of filter topologies for passive filter applications," *IEEE Trans. Power Deliv.*, vol. 24, no. 3, pp. 1710–1718, 2009.

[21] A. K. Mishra, P. K. Nanda, D. Das, A. K. Patra, N. Nahak, and L. M. Sathapathy, "Design and Analysis of Shunt Passive Filter for Harmonic and Reactive Power Compensation," in *2023 International Conference in Advances in Power, Signal, and Information Technology, APSIT, India, 2023*, 2023, pp. 347–352. doi: 10.1109/APSIT58554.2023.10201759.

[22] F. Zaro, "Power Quality Improvement using Shunt Active Power Filter: An Industrial Zone Case Study," *WSEAS Transactions on Power Systems*, vol. 18, pp. 179-185, 2023, doi: 10.37394/232016.2023.18.19.

[23] F. Zaro, "Shunt Active Power Filter for Power Quality Improvement of Renewable Energy Systems: A Case Study," *WSEAS Transactions on Power Systems*, vol. 18, no. 14, pp. 241-247, 2023, doi: 10.37394/232016.2023.18.25.

[24] A. Bouhouta, S. Moulahoum, N. Kabache, A. Moualdia, and I. Colak, "Harmonics Compensation of Grid-Connected PV Systems Using a Novel M5P Model Tree Control," in *11th International Conference on Smart Grid, icSmartGrid,Parie France, 2023*, 2023, pp. 1–6. doi: 10.1109/icSmartGrid58556.2023.10170901.

[25] A. M. Sharaf, F. H. Gandoman, and B. Khaki, "Active harmonic filters," *Power Qual. Futur. Electr. Power Syst.*, vol. 93, no. 12, pp. 131–163, 2017, doi: 10.1049/pbpo092e_ch4.

[26] O. T. Ibitoye, M. O. Onibonoje, and J. O. Dada, "Analysis of Power Quality and Technical Challenges in Grid-Tied Renewable Energy," *WSEAS Transactions on Power Systems*, vol. 18, no. 608, pp. 248–258, 2023, doi: 10.37394/232016.2023.18.26.

[27] Q. Jin, Z. Yao, and M. Guo, "A Control Method of Shunt Active Power Filter for System-wide Harmonic Suppression Based on Complex-valued Neural Network," in *2020 IEEE 9th International Power Electronics and Motion Control Conference, IPEMC ECCE Asia,Nanjing, China,2020*, 2020, pp. 1543–1548. doi: 10.1109/IPEMC-ECCEAsia48364.2020.9368080.

[28] A. Y. Hatata, M. Eladawy, and K. Shebl, "Parameter control scheme for active power filter based on NARX neural network," *WSEAS Transactions on Power Systems*, vol. 13, no. Pt 1, pp. 118–124, 2018.

[29] P. P. Behera, D. A. Gadanayak, R. R. Panigrahi, and M. Mishra, "A Mamdani Type Fuzzy Controller with Mathematical Morphology for Shunt Active Power Filters," in *2023 1st International Conference on Circuits, Power, and Intelligent Systems, CCPIS,Bhubaneswar, India, 2023*, 2023, pp. 1–5. doi: 10.1109/CCPIS59145.2023.10291823.

[30] S. Othman, M. A. Alali, L. Sbita, J. P. Barbot, and M. Ghanes, "Modeling and control design based on petri nets tool for a serial three-phase five-level multicellular inverter used as a shunt active power filter," *Energies*, vol. 14, no. 17, 2021, doi: 10.3390/en14175335.

[31] S. Othman, J. P. Barbot, L. Sbita, M. A. Alali, M. Ghanes, and A. Fekik, "Hybrid renewable energy system based on Petri nets control for a single-phase flying capacitor multilevel DC–AC converter," in *Power Electronics Converters and their Control for Renewable Energy Applications*, A. Fekik, M. Ghanes, and H. Denoun, Eds., Academic Press, 2023, pp. 145–166. doi: 10.1016/B978-0-323-91941-8.00007-X.

[32] M. N. Iqbal, L. Kutt, B. Asad, and N. Shabbir, "Impact of cable impedance on the harmonic emission of LED lamps," in *Proceedings - 2020 21st International Scientific Conference on Electric Power Engineering, EPE, Prague, Czech Republic, 2020*, 2020, pp. 1–5. doi: 10.1109/EPE51172.2020.9269271.

Contribution of Individual Authors to the Creation of a Scientific Article (Ghostwriting Policy)

The authors equally contributed to the present research, at all stages from the formulation of the problem to the final findings and solution.

Sources of Funding for Research Presented in a Scientific Article or Scientific Article Itself

No funding was received for conducting this study.

Conflict of Interest

The authors have no conflicts of interest to declare.